THE ASTROPHYSICAL JOURNAL, 234:L117–L122, 1979 December 1

X AND UV RADIATION FROM ACCRETING MAGNETIC DEGENERATE DWARFS[1]

D. Q. LAMB,[2] AND A. R. MASTERS
Department of Physics,
University of Illinois at Urbana-Champaign
Received 1979 June 4; accepted 1979 August 9

ABSTRACT

We have carried out detailed numerical calculations of high-harmonic cyclotron emission from a hot plasma, and from these calculations we have developed a self-consistent, quantitative model of X-ray and UV emission from accreting magnetic degenerate dwarfs. We find that such stars are typically strong UV sources, and emit only a small fraction of their luminosity in soft and hard X-rays. The qualitative features of the X and UV spectra suffice to determine the mass, magnetic field strength, and luminosity of the source with relative confidence. Our results show that the soft and hard X-ray emission observed from AM Her, AN UMa, and 3A 0211−227 are typical of these objects.

Subject headings: stars: accretion — stars: magnetic — stars: white dwarfs — ultraviolet: spectra — X-rays: spectra

I. INTRODUCTION

The discovery that AM Her is a source of soft and hard X-rays (Hearn, Richardson, and Clark 1976; Berg and Duthie 1977) and is strongly magnetic (Tapia 1977*a*) has led to the recognition that accreting magnetic degenerate dwarfs comprise an important class of galactic X-ray sources. The distances to AM Her and to known similar sources indicate that the space density of these sources is $\gtrsim 10^{-7}$ pc^{-3} and that their total number in the galaxy is $\gtrsim 10^5$.

Accreting magnetic degenerate dwarfs were expected to be sources of intense UV and, possibly, X-ray emission (Bath, Evans, and Pringle 1974; Lamb 1974). Fabian, Pringle, and Rees (1976) and Masters *et al.* (1977) have discussed the qualitative features of such emission using results available from earlier studies of cyclotron emission in plasma fusion devices utilizing magnetic confinement (see Bekefi 1966 for an excellent review). They were unable to obtain quantitative results, however, because knowledge of the cyclotron emissivity at high harmonics was lacking. In this *Letter*, we report the results of detailed numerical calculations of high-harmonic cyclotron emission from a hot plasma, and present a self-consistent, quantitative model of X-ray and UV emission from accreting magnetic degenerate dwarfs.

We briefly describe our calculations in § II, discuss the results in § III, and remark on the implications for observed X-ray sources in § IV. Full details of our calculations and a more complete discussion of our results will be given elsewhere (Lamb and Masters 1979).

[1] This research was supported in part by NSF grant PHY78-04404 and NASA contract NAS5-11450.

[2] John Simon Guggenheim Memorial Fellow. Also Department of Physics, Massachusetts Institute of Technology.

II. CALCULATIONS

a) High-Harmonic Cyclotron Emission from a Hot Plasma

The size parameter $\Lambda \equiv \omega_p^2 l/\omega_c c$, where ω_p is the electron plasma frequency, ω_c is the cyclotron frequency, and l is the length scale of interest, is a rough measure of the optical depth at the cyclotron fundamental (Trubnikov 1958). In the emission regions of accreting magnetic degenerate dwarfs, Λ may easily reach 10^9 (Masters *et al.* 1977). Then only above some energy $E^* = \hbar\omega^*$, where ω^* may exceed, say, the 50th harmonic, is the source optically thin and is the emitted flux optically thin cyclotron emission. Below E^* the source is heavily self-absorbed and the emitted flux is limited to the Rayleigh-Jeans tail of a blackbody spectrum having a temperature equal to the electron temperature T_e. Thus neither the optically thin cyclotron spectrum nor the blackbody spectrum gives an adequate representation of the spectrum actually emitted, and hence of the cyclotron cooling rate. Instead, one must have accurate knowledge of the cyclotron emissivity at high harmonics and then find the value of E^*, and hence the cyclotron cooling rate, by treating the frequency-dependent radiative transfer within the emission region.

As a first step, we have therefore carried out accurate calculations of the cyclotron emissivity at high harmonics (Lamb and Masters 1979; see also Masters 1978). An example of our results is shown in Figure 1. The dimensionless flux $\Phi(z, \theta)$ shown is the cyclotron emissivity normalized to the Rayleigh-Jeans spectral flux in a single polarization (see Hirschfield, Baldwin, and Brown 1961). It is a function only of $\theta = kT_e/m_e c^2$ and $z = \omega/\omega_c$. With this normalization, E^* for a particular emission region having a size parameter Λ is just given by that z for which $\Lambda\Phi = 1$. All the

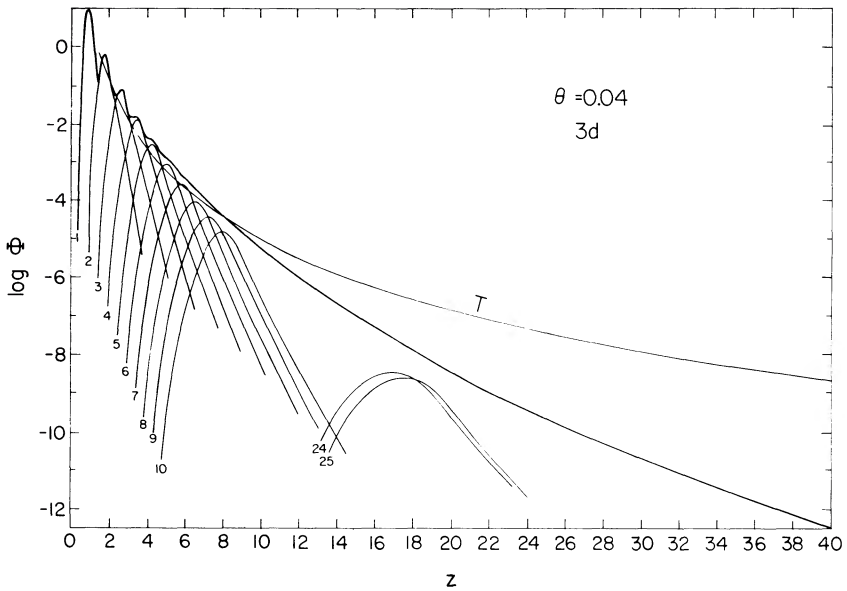

FIG. 1.—Dimensionless spectral flux Φ from a three-dimensional distribution of electrons with $\theta = 0.04$. The heavy curve is the total flux; the light curves are the individual harmonics. Note that the peak of the nth harmonic lies increasingly farther below nz as n becomes large. The curve labeled "T" is the fit obtained by Trubnikov (1973).

dependence on the density and geometry of the emission region is contained in the size parameter Λ. Figure 1 shows the cyclotron spectral flux from an optically thin plasma with electron temperature $T_e = 20$ keV. The heavy curve shows the total spectral flux, while the light curves show the contributions of individual harmonics. The radiation at high harmonics is due primarily to electrons in the high-velocity tail of the Maxwellian distribution. At the mildly relativistic temperatures of interest here, γ is appreciably greater than one for electrons in this tail. Therefore, the peak of the nth harmonic lies increasingly farther below nz as n becomes large. The curve labeled "T" shows the fit obtained by Trubnikov (1972) to calculations by Drummond and Rosenbluth (1963) for the range $5 < z < 10$. The agreement with our calculations is encouraging there, but the necessity of new calculations is evident from the fact that this fit already differs from the actual Φ by $\sim 10^4$ when $z \approx 40$. Figure 1 illustrates three important features of the cyclotron emissivity: namely, most of the emission occurs above the fundamental if the temperature is moderate or high, the emissivity falls steeply with frequency, and thermal broadening of the individual harmonics produces a smooth continuum at high frequencies.

b) Assumptions

The calculations of X-radiation from magnetic degenerate dwarfs that we will discuss here assume (1) steady, radial accretion over a fractional area f of the stellar surface; (2) a magnetic field; (3) complete ionization of the accreting matter; (4) no nuclear burning; and (5) an idealized emission region.

Accretion over only a fraction of the stellar surface takes into account the possibility that matter is channeled onto the magnetic poles by the magnetic field. As in the case of nonmagnetic degenerate dwarfs, the accreting matter is often expected to be strongly photoionized. Any absorption will then occur far away from the X-ray source, and if $f \ll 1$, such absorption will have little importance except when the line of sight from the emission region to the observer lies directly in the column of accreting matter. If nuclear burning occurs, it will produce a large blackbody flux. Unlike the case of nonmagnetic degenerate dwarfs, it may do little else, since in general cyclotron cooling, rather than Compton cooling resulting from the enhanced blackbody flux, will remain the dominant cooling mechanism in the emission region.

Rather than attempt to solve the full coupled hydrodynamic and frequency-dependent radiative transfer problem, which would determine completely the structure of the hot, postshock emission region and the shape and angular dependence of the emitted flux, we idealized the emission region as follows. The emission region is assumed to be a geometrically thin slab[3] having uniform temperature and density. These assumptions will be roughly correct as long as the shock standoff distance $d < R$, and $d \ll (2f)^{1/2}R$ so that the area of the slab's face is larger than that of its edges. Coulomb collisions are assumed to be the only electron-ion energy-exchange mechanism. Variations and anisotropies in the emission and absorption of cyclotron radiation are neglected, and a total cyclotron cooling rate is used instead. This rate corresponds to emission equal to the appropriate Rayleigh-Jeans

[3] The calculations can be extended in a straightforward fashion to the opposite geometry of a tall, thin cylinder if the temperature, density, and magnetic field strength are assumed to be uniform in the emission region.

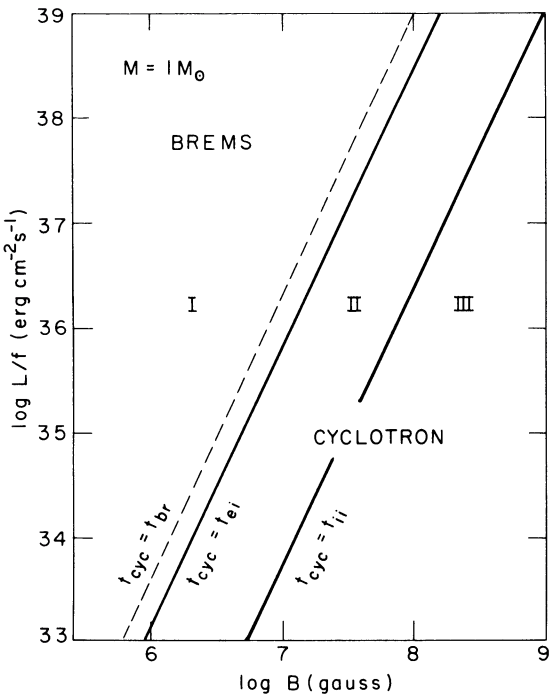

FIG. 2.—Parameter regimes in the (B, L/f)-plane for an $M = 1.0\ M_\odot$ star. The one-fluid regime lies above and to the left of the solid line labeled $t_{cyc} = t_{ei}$, the two-fluid regime below and to the right. The nonhydrodynamic regime lies below and to the right of the solid line labeled $t_{cyc} = t_{ii}$. Cyclotron emission dominates below and to the right of the dashed line, bremsstrahlung above and to the left. The solid curves labeled $t_{cyc} = t_{ei}$ and $t_{cyc} = t_{ii}$ divide accretion onto magnetic degenerate dwarfs into three parameter regimes, labeled I, II, and III.

spectrum below E^* and to an optically thin cyclotron spectrum above E^*. These assumptions allow the important parameter regimes to be delineated and approximate spectra to be calculated.

c) *Parameter Regimes*

With the above assumptions, a picture of X-ray emission by magnetic degenerate dwarfs emerges that is analogous to that for nonmagnetic degenerate dwarfs (Kylafis and Lamb 1979, and references therein). As accreting matter flows toward the star, a strong standoff shock forms far enough above the star for the hot, postshock matter to cool and come to rest at the stellar surface (Fabian, Pringle, and Rees 1976). The standoff distance $d \equiv r_s - R \approx \frac{1}{4} v_{ff}(r_s) t_{cool}(r_s)$, where r_s is the shock radius, R is the stellar radius, v_{ff} is the free-fall velocity, and t_{cool} is the time scale for cooling, due now to both bremsstrahlung and cyclotron emission. Roughly half of the cyclotron flux is emitted outward and forms a blackbody-limited component in the UV. Roughly half of the bremsstrahlung flux is emitted outward and forms a hard X-ray component. The other halves of the cyclotron and bremsstrahlung fluxes are emitted inward and are reflected or absorbed by the stellar surface. The resulting blackbody flux forms a UV or soft X-ray component with $L_{bb} \approx L_{cyc} + L_{br}$, where L_{bb}, L_{cyc}, and L_{br} are the luminosities in the blackbody, cyclotron, and bremmstrahlung components.

The effective accretion rate of the accreting sector is $\dot{M}/f$, and the corresponding luminosity is L/f. X-radiation and UV-radiation from magnetic degenerate dwarfs are thus functions of stellar mass M, magnetic field strength B, and effective luminosity L/f. (Note that in some circumstances f may be a function of B.) The dependence on stellar mass is significant but is less than on the other two variables. If we specify the mass of the star, the parameter regimes encountered are conveniently displayed on a (B, L/f)-plane as shown for a 1 $M_\odot$ star in Figure 2. The upper left of the plane corresponds to low magnetic field strengths and high effective luminosities (and thus high densities in the emission region). In this portion of the plane, bremsstrahlung cooling dominates cyclotron cooling in the hot, postshock emission region, and the results for nonmagnetic degenerate dwarfs apply. As one increases B or lowers L/f, moving toward the lower right in Figure 2, cyclotron cooling becomes more important until eventually it dominates (Masters *et al.* 1977). The dashed line shows the location at which this occurs, as determined from detailed numerical calculations equating t_{cyc} and t_{br}, the cyclotron and bremsstrahlung cooling time scales.

As long as bremsstrahlung emission dominates, electrons and ions generally exchange energy faster than the rate at which the electrons lose energy. The electrons and ions in the hot, postshock emission region are then able to achieve a single temperature and may be treated as a single fluid. On the other hand, if cyclotron emission dominates, the rate at which the electrons are cooled can be rapid enough to prevent their ever achieving a common temperature with the ions (Fabian, Pringle, and Rees 1976). The electrons and ions must then be treated as two separate fluids. The transition between the one- and two-fluid regimes occurs when the cyclotron cooling time scale t_{cyc} equals the electron-ion energy-exchange time scale t_{ei}, and is shown as a solid line in Figure 2.

As one moves further toward the lower right in Figure 2, the cyclotron cooling rate becomes so great that the ions lose their energy to the electrons before the ions have sufficient time to form a Maxwellian velocity distribution via Coulomb collisions among themselves. The behavior of the ions is then no longer hydrodynamic, and new methods must be introduced to treat the problem. The onset of the nonhydrodynamic regime occurs when the cyclotron cooling time scale t_{cyc} equals the ion-ion energy-exchange time scale t_{ii}, and is also shown by a solid line in Figure 2.

As one moves still further toward the lower right in Figure 2, two other effects become important. First, the high-energy tail of the electron-velocity distribution, which is responsible for the bulk of cyclotron emission at high harmonics, may be depopulated so rapidly by cyclotron emission that Coulomb collisions are unable to sustain it. The rate of cyclotron emission is then altered. Second, cyclotron emission reduces the component of electron velocity perpendicular to the magnetic field. This reduction may become so rapid

that Coulomb collisions are unable to sustain an isotropic electron velocity distribution ($t_{cyc} \ll t_{ee}$). However, both of these effects become important only after the onset of nonhydrodynamic behavior by the ions.

The solid curves labeled $t_{cyc} = t_{ei}$ and $t_{cyc} = t_{ii}$ divide accretion onto magnetic degenerate dwarfs into three parameter regimes, labeled I, II, and III.

III. RESULTS

a) Spectrum

The X and UV spectra produced by accretion onto magnetic degenerate dwarfs generally have 4 components: (1) a blackbody-limited UV cyclotron component produced by the hot emission region; (2) a hard X-ray bremsstrahlung component also produced by the hot emission region; (3) a hard UV or soft X-ray blackbody component produced by cyclotron and bremsstrahlung photons that are absorbed by the stellar surface and re-emitted; and (4) secondary radiation from infalling matter above the shock or, possibly, from the stellar surface around the emission region. The first three components are clearly visible in Figure 3, which shows the X and UV spectra from the emission region alone produced by accretion at two different rates, corresponding to $L/f = 10^{35}$ and 10^{37} ergs s^{-1}, onto a 1.0 $M_\odot$ star having a magnetic field of 2×10^7 gauss. Since secondary radiation is not included, the portion of each spectrum below ~5 eV is less certain.

From the spectra illustrated in Figure 3 we draw two important conclusions. First, magnetic degenerate dwarfs are predicted to be strong UV sources with only a few percent of the total accretion luminosity ordinarily appearing as soft and hard X-rays, and therefore accessible to existing detectors. Second, the position and relative strength of the spectral components change with variations in the accretion rate. For example, with the change in accretion rate shown, the blackbody component moves from the UV into the soft X-ray region, and the luminosity of the bremsstrahlung hard X-ray component increases by nearly four orders of magnitude while the total accretion luminosity is increasing by only two.

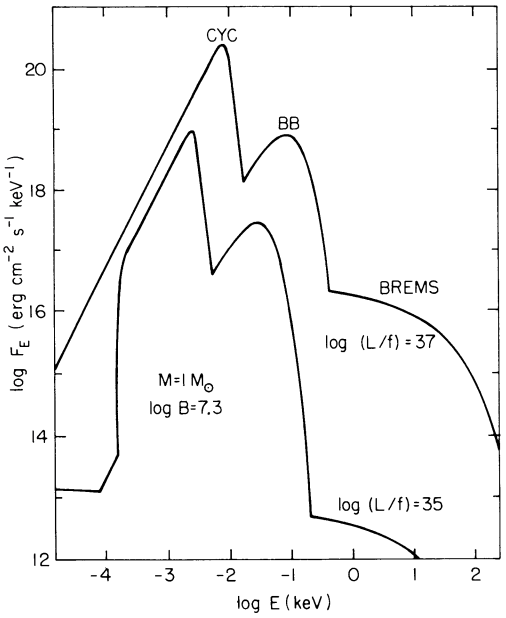

FIG. 3.—X-ray and UV spectrum produced by two different accretion rates onto a 1 $M_\odot$ degenerate dwarf having a magnetic field of $B = 2 \times 10^7$ gauss. The portion of each spectrum below ~5 eV is less certain due to possible secondary radiation.

The parameters of the spectra shown in Figure 3 are as follows. For the low-luminosity example, which belongs to regime II, the bremsstrahlung component has a temperature $T_e = 21.0$ keV, the blackbody component has a temperature $T_{bb} = 10.6$ eV, and the peak of the blackbody-limited cyclotron component occurs at $E^* = 2.85$ eV. For the high-luminosity example, which belongs to regime I, $T_e = 56.2$ keV, $T_{bb} = 32.2$ eV, and $E^* = 9.05$ eV. The ratio of the cyclotron luminosity to the bremsstrahlung luminosity, $q = L_{cyc}/L_{br}$, signals whether one is in regime I or II, with $q \ll 10$ indicating regime I and $q \gg 10$ indicating regime II for a 1 $M_\odot$ star. Thus $q = 2.75$ and 334 for the high- and low-luminosity spectra, respectively.

We expect $f \ll 1$ for most magnetic degenerate dwarfs. Since the hot, postshock emission region is then small and both the cyclotron and blackbody components are blackbody-limited at low energies, the visual characteristics of most such stars are very likely *not* dominated by flux from the emission region. Instead, the flux observed in the visual is very likely dominated by secondary radiation; that is, either by emission from infalling matter, above the shock, that is heated by Compton scattering or cyclotron absorption (cf. Chanmugam and Wagner 1977; Stockman *et al.* 1977) or, possibly, by emission from the stellar surface, surrounding the emission region, that is heated by radiative transfer.

b) Correlation between Spectral Temperature, Luminosity, and Magnetic Field Strength

Unlike the case of nonmagnetic degenerate dwarfs, where the shapes and strengths of the spectral components are a function only of mass accretion rate (Kylafis and Lamb 1979), here they depend on both mass accretion rate and magnetic field strength. Spectral variations are therefore best displayed by plotting the contours of quantities of interest on a $(B, L/f)$-plane. A set of such contours is plotted in Figure 4 for a 1.0 $M_\odot$ star. Figure 4 shows that observation of the qualitative features of the spectrum is sufficient to determine with relative confidence the physical conditions in the X-ray emission region, including the value of the magnetic field. The cyclotron component is ordinarily, and the blackbody component may frequently be, inaccessible to existing detectors. Nevertheless, optical, soft X-ray, and hard X-ray observations will often be sufficient to determine the mass and magnetic field of the star, and its accretion rate. For example, observation of T_e and T_{bb} fixes a

point in the (B, L/f)-plane of Figure 4 and also constrains the star to a limited range of masses. Measurement of E^*, q, or a constraint from optical observations then tests the consistency, and hence validity, of the basic model. Furthermore, if an independent estimate of f exists, the intrinsic luminosity L is then known, as is the distance of the source.

IV. DISCUSSION

a) *Implications for Observed Sources*

AM Her shows strong circular polarization ($\gtrsim 10\%$) at visual wavelengths (Tapia 1977*a;* Stockman and Sargent 1979), and is believed to be an accreting magnetic degenerate dwarf (Chanmugam and Wagner 1977, 1978*;* Stockman *et al.* 1977; Priedhorsky and Krzeminski 1978). AN UMa and VV Puppis also show strong circular polarization at visual wavelengths (Tapia 1977*b;* Krzeminski and Serkowski 1977; Liebert *et al.* 1978; Liebert and Stockman 1979), and recently AN UMa has been detected in soft X-rays (Hearn and Marshall 1979). Furthermore, the weak, hard X-ray source 2A 0311−227 has recently been found to be a soft X-ray source (Hearn 1979*a*, *b;* Charles, Mason, and Bowyer 1979) and to exhibit strong circular polarization at visual wavelengths (Tapia 1979). All of these AM Her systems can be interpreted in terms of our model.

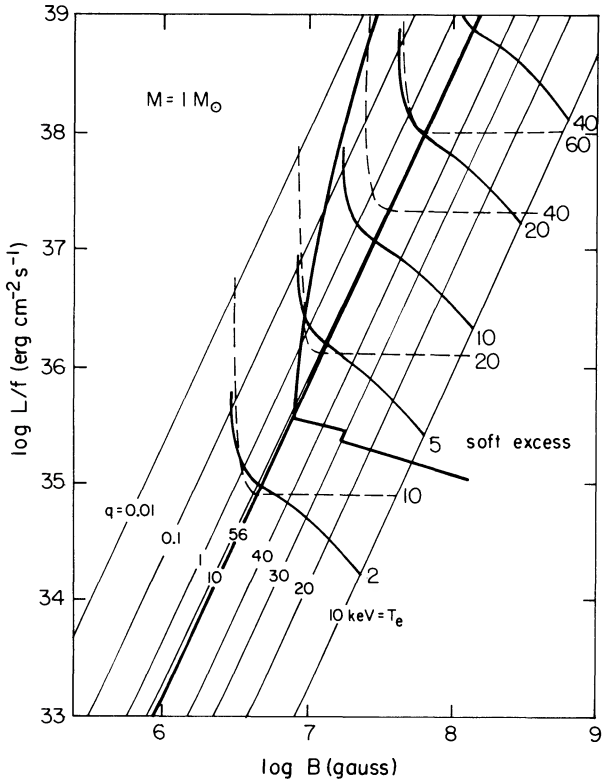

FIG. 4.—Temperature and luminosity contours in the (B, L/f) plane for an $M = 1.0\ M_\odot$ star. The regions where bremsstrahlung and cyclotron emission dominate are the same as in Fig. 2. Contours of constant E^* (in eV) are shown as thick solid lines and those of constant T_{bb} (in eV) as dashed lines. The thin solid lines in the bremsstrahlung-dominated region show contours of constant q, while those in the cyclotron-dominated region show contours of constant T_e (in keV). The very thick diagonal line marks the boundary between regimes I and II. The spectral flux of the blackbody component exceeds that of the bremmstrahlung component at 0.25 keV to the right and above the very thick line labeled "soft excess." Near and above $L/f = L_E/f = 1.4 \times 10^{33}$ ergs s^{-1}, radiation pressure can be important and modify the results, but because photons can easily scatter out of the accretion column if $f \ll 1$, the Eddington luminosity does not represent the stringent upper limit to the luminosity that it does in the case of nonmagnetic degenerate dwarfs. Below and to the left of the curve $E^* = 2$ eV, the assumption $d < R$ breaks down. In both of these regions, the values shown are expected to remain qualitatively correct.

Soft X-ray observations (Hearn, Richardson, and Clark 1976; Hearn and Richardson 1977; Bunner 1978; Tuohy *et al.* 1978) and hard X-ray observations (Swank *et al.* 1977; Staubert *et al.* 1978) of AM Her show two distinct components with temperatures $\sim$30 keV[4] and $\lesssim$40 eV. Tuohy *et al.* (1978) have shown that, if these two components are interpreted as the bremsstrahlung and blackbody components predicted in our model, the observed optical flux requires $T_{bb} \gtrsim 25$ eV. Assuming $M = 1\ M_\odot$, AM Her is then constrained to have $B \sim 10^8$ gauss and $L/f \sim 10^{37}$ ergs s^{-1} (see Fig. 4). However, recent UV observations (Treves 1978; Raymond *et al.* 1979) find a flux an order of magnitude less than these parameters predict. One possible explanation is that AM Her has a lower magnetic field than previously thought; say, 3×10^7 gauss. This would lower E^* and reduce L_{cyc} relative to L_{br}, thereby resolving the conflict with the UV observations. However, the strength of the optical polarization ($\gtrsim 10\%$) then presents some difficulties.

DQ Her is also believed to be an accreting magnetic degenerate dwarf (Lamb 1974; Bath, Evans, and Pringle 1974). This system underwent a nova outburst in 1934 and shows coherent, small-amplitude, optical pulsations at 71 s. V533 Her, which underwent a nova outburst in 1963 and shows coherent small-amplitude optical pulsations at 63 s (Patterson 1979*a*), is almost certainly a similar system. Another member of this class is AE Aqr, which shows coherent optical pulsations at 33 s (Patterson 1979*b*). In each case, the period of the coherent optical pulsations is believed to represent the rotation period of the degenerate dwarf. Unlike the AM Her systems, none of the DQ Her systems have been detected in soft or hard X-rays, and DQ Her shows only a small amount of circular polarization at optical wavelengths (Swedlund, Kemp, and Wolstencroft 1974). Furthermore, all of these systems exhibit clear optical evidence of an accretion disk and none have rotation periods synchronized with the binary orbital period. All of these differences from the AM Her systems suggest that the degenerate dwarfs in the DQ Her systems have weaker magnetic fields and, con-

[4] Staubert *et al.* (1978) fitted an 18 keV exponential spectrum to their hard X-ray data and that of Swank *et al.* (1977). Note, however, that a thin bremsstrahlung spectrum *including Gaunt factor* fits the combined data very poorly.

comitantly, lower values of L/f. The weaker magnetic field is less able to enforce synchronous rotation of the degenerate dwarf and to prevent formation of a disk. The lower values of B and L/f make the copious production of soft and hard X-rays more difficult.

It is a pleasure to thank Fred Lamb for valuable discussions on the physics of X-ray emission from degenerate stars and Dave Hearn, Jim Liebert, John Raymond, Pete Stockman, and Aldo Treves for extensive discussions on the observations.

REFERENCES

Bath, G. T., Evans, W. D., and Pringle, J. E. 1974, *M.N.R.A.S.*, **166**, 113.
Bekefi, G. 1966, *Radiation Processes in Plasmas* (New York: Wiley).
Berg, R. P., and Duthie, J. G. 1977, *Ap. J.*, **211**, 859.
Bunner, A. N. 1978, *Ap. J.*, **220**, 261.
Chanmugam, G., and Wagner, R. L. 1977, *Ap. J.* (*Letters*), **213**, L13.
———. 1978, *Ap. J.*, **222**, 641.
Charles, P. A., Mason, K. O., and Bowyer, S. 1979, *IAU Circ.*, No. 3329.
Drummond, W. E., and Rosenbluth, M. N. 1963, *Phys. Fluids*, **6**, 276.
Fabian, A. C., Pringle, J. E., and Rees, M. J. 1976, *M.N.R.A.S.*, **173**, 43.
Hearn, D. R. 1979*a*, *IAU Circ.*, No. 3326.
———. 1979*b*, *IAU Circ.*, No. 3327.
Hearn, D. R., and Marshall, F. J. 1979, *Ap. J.* (*Letters*), **232**, L21.
Hearn, D. R. and Richardson, J. A. 1977, *Ap. J.* (*Letters*), **213**, L115.
Hearn, D. R., Richardson, J. A., and Clark, G. W. 1976, *Ap. J.* (*Letters*), **210**, L23.
Hirschfield, J. L., Baldwin, D. E., and Brown, S. C. 1961, *Phys. Fluids*, **4**, 198.
Krzeminski, W., and Serkowski, I. 1977, *Ap. J.* (*Letters*), **216**, L45.
Kylafis, N. D., and Lamb, D. Q. 1979, *Ap. J.* (*Letters*), **228**, L105.
Lamb, D. Q. 1974, *Ap. J.* (*Letters*), **192**, L129.
Lamb, D. Q., and Masters, A. R. 1979, in preparation.
Liebert, J., and Stockman, H. S. 1979, *Ap. J.*, **229**, 652.
Liebert, J., Stockman, H. S., Angel, J. R. P., Woolf, N. J., Hege, K., and Margon, B. 1978, *Ap. J.*, **225**, 201.
Masters, A. R. 1978, Ph.D. thesis, University of Illinois.
Masters, A. R., Fabian, A. C., Pringle, J. E., and Rees, M. J. 1977, *M.N.R.A.S.*, **178**, 501.
Patterson, J. 1979*a*, *Ap. J.*, **231**, 789.
———. 1979*b*, *Ap. J.*, **234**, in press.
Priedhorsky, W. C., and Krzeminski, W. 1978, *Ap. J.*, **219**, 597.
Raymond, J. C., Black, J. H., Davis, R. J., Dupree, A. K., Gursky, H., Hartmann, L., and Matilsky, T. A. 1979, *Ap. J.* (*Letters*), **230**, L95.
Staubert, R., Kendziorra, E., Pietsch, W., Reppin, C., Trumper, J., and Voges, W. 1978, *Ap. J.* (*Letters*), **225**, L113.
Stockman, H. S., and Sargent, T. A. 1979, *Ap. J.*, **227**, 197.
Stockman, H. S., Schmidt, G. D., Angel, J. R. P., Liebert, J., Tapia, S., and Beaver, E. A. 1977, *Ap. J.*, **217**, 815.
Swank, J., Lampton, M., Boldt, E. M., Holt, S., and Serlemitsos, P. 1977, *Ap. J.* (*Letters*), **216**, L71.
Swedlung, J. B., Kemp, J. C., and Wolstencroft, R. D. 1974, *Ap. J.* (*Letters*), **193**, L11.
Tapia, S. 1977*a*, *Ap. J.*, **212**, L125.
———. 1977*b*, *IAU Circ.*, No. 3054.
———. 1979, *IAU Circ.*, No. 3327.
Treves, A. 1978, private communication.
Trubnikov, B. A. 1958, AEC-tr-4073 (Washington: Office of Technical Services).
———. 1972, *Zh. ETF Pis. Red.*, **16**, 37 (Eng. transl. [1973] Soviet Phys.—JETP, **16**, 25).
Tuohy, I. R., Lamb, F. K., Garmire, G. P., and Mason, K. O. 1978, *Ap. J.* (*Letters*), **226**, L17.

D. Q. Lamb: Department of Physics, Massachusetts Institute of Technology, Cambridge, MA 02139

A. R. Masters: Shell Development Corporation, P.O. Box 481, Houston, TX 77001